Synthesis, processing, and migration of a 2D data from the Gulf of Mexico

Huy Le, Stewart A. Levin, and Robert G. Clapp

ABSTRACT

As a step toward applying our anisotropic waveform inversion methodology developed and presented in previous reports, we synthesized a 2D seismic data set from a 3D cross-shooting data acquired offshore Gulf of Mexico. The data's cross-shooting geometry poses a challenge to 2D processing and migration. Since the source lines and receiver lines are perpendicular, out-of-plane events could degrade image quality. Additionally, there are a number of salt bodies in the data area, which, at some locations, rise up to sea bottom with steep flanks causing imaging problems with short-offset data. We migrated the resulting 2D data with an isotropic velocity. Despite all the limitations, we were able to image reflectors down to four kilometers depth. However, segments of the salt bodies' boundaries could hardly be traced due to low signal to noise ratio in deeper portions of the data.

INTRODUCTION

In previous reports, we implemented a time-domain anisotropic full-waveform inversion (FWI) method using second-order pseudo-acoustic wave equations in transverse isotropic media and applied it to synthetic models and data (Le, 2016a,b). Our next step is to test our implementation on a field data set. Among data donated to SEP by our sponsors, the E-Dragon data caught our attention. The data area is rich in shale and layered in many places, which makes it suitable for anisotropic imaging and inversion. Alignment of clay minerals in shale and layering combine to create a medium of at least transverse isotropy. Moreover, salt bodies' movement could potentially cause stress anomalies, which further lowers the medium's symmetry to, e.g., orthorhombic. Isotropic imaging applied to areas that display anisotropy can result in poor focus and wrong placement of reflectors.

Anisotropic model building is a challenging problem because of the large number of unknown parameters, their trade-offs, and uncertainty. In order to constrain anisotropic inversion, additional sources of information should be incorporated. E-Dragon data come together with well logs, mud weights, and attribute cubes, such as shale volume, pore pressure, and effective stress, which makes is possible to explore different types of constraints. The availability of data from E-Dragon has promoted the work of a former SEP student, Elita Li (Li et al., 2016), who used geological and

rock physics constraints in Wave Equation Migration Velocity Analysis (WEMVA). In another paper in this report, we develop a workflow that use geomechanical information and basin modeling for constraining anisotropic FWI.

ACQUISITION AND PROCESSING

The data set we chose was acquired in the Gulf of Mexico at four millisecond sampling, using ocean bottom cables (OBC). The area where it was recorded has a shallow water depth, approximately 36 meters on average. We were provided with P-Z summed data. Figures 1a and 1b respectively show the source locations and receiver locations. The source lines are perpendicular to the receiver lines. Source line spacing is 400 meters and source spacing is 50 meters, while receiver line spacing is 600 meters and receiver spacing is 50 meters. Maximum offset is about six kilometers.

To synthesize a 2D data set from the original 3D data, we chose a subset of the 3D data with midpoints within a one-kilometer swath, covering two receiver lines. These receiver lines are in close proximity to one of the wells in the survey area and overlay interesting salt bodies that we hope to image. Figure 2a shows locations of the midpoints, two receiver lines, and corresponding sources.

Assuming structures and velocity do not vary significantly in the cross-line direction, the chosen sources and recievers were rotated about their midpoints to align in-line. Figure 2b shows locations of the sources and receivers after rotation. Rotated sources and receivers densely cover a patch one kilometer wide and 30 kilometers long, which we will regard as our 2D data. The rotation is trusted to not change reflection moveouts because the water depth at this area is particularly shallow. As a result, no differential moveout correction was applied. The resulting data were then sorted into 50-meter bins and stacked. This produces 536 shots, of which only one quarter is used for migration. We also applied a low-pass 30 Hz filter to the data. Figures 3a and 3b show two sample shots. Some reflection hyperbolas are identifiable in the first four seconds of the data. Little coherent signal shows in the later parts of the data.

MIGRATION

The data came with an isotropic velocity model that was obtained with ray-based tomography. Figure 4a shows a 2D section of the velocity model along our synthesized 2D line. The velocity section shows monotonic variation with depth down to about four kilometers, but changes laterally in deeper regions, especially around salt bodies. Those are areas we expect our 2D approximation and rotation break down. Figure 4b shows the same 2D velocity section, in which the salt bodies were already removed and filled with surrounding sediment velocity. This is our migration velocity.

We performed isotropic migration on the synthesized data using a Ricker wavelet of 10 Hz central frequency. Figure 5 shows the migrated image. As expected, we

observed a number of continuous and relatively flat reflectors down to four kilometers. The image degrades below that. This is due to low data quality and inaccuracy of our 2D assumption. This is also where the salt bodies locate and velocity significantly changes laterally. Consequently, we were able to image only segments of the salt bodies at around seven kilometer depth.

Figures 6 and 7 show angle gathers at various locations. A number of reflectors with downward curvatures can be identified. This indicates our migration velocity might be faster than true velocity. This is because isotropic ray-based tomography tends to capture normal moveout velocity, which, in areas of positive ϵ, is greater than vertical velocity. This leaves room for improvement with anisotropic velocity models that we hope to build.

CONCLUSIONS

We synthesized a 2D data set from cross-shooting 3D data from the Gulf of Mexico. We chose an area that has interesting salt structures and is close to wells that can be used later in the inversion process. With an isotropic velocity model, we were able to image sedimentary layers above the salt bodies. Even though the image degrades in the deeper half, segments of the salt boundaries were visible. The angle gathers display downward curvatures on a number of reflectors, indicating that the migration velocity is higher than true velocity. This is where our anisotropic FWI tools can help to build a better velocity model and improve these angle gathers.

ACKNOWLEDGEMENT

We would like to thank Schlumberger MultiClient for providing us the field data. We also thank Professor Biondo Biondi, Huy Le's thesis advisor, for many insightful discussions.

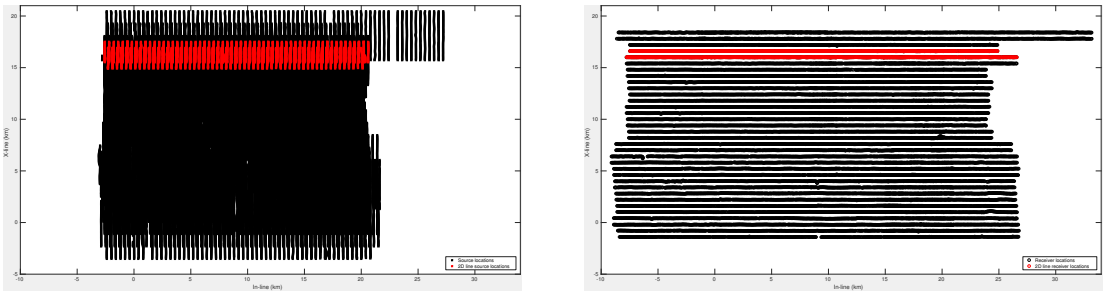

(a) (b)

Figure 1: Source (left) and receiver (right) locations of the original 3D data set and location of the picked 2D line (in red). [**ER**]

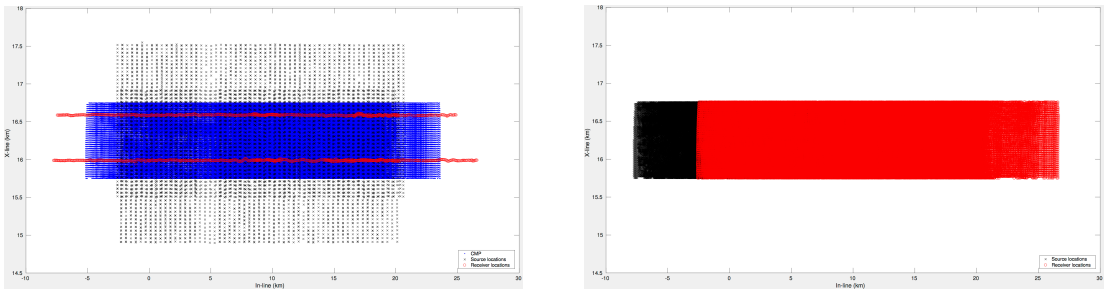

(a) (b)

Figure 2: Source, receiver, and midpoint locations before (left) and after (right) rotation. [**ER**]

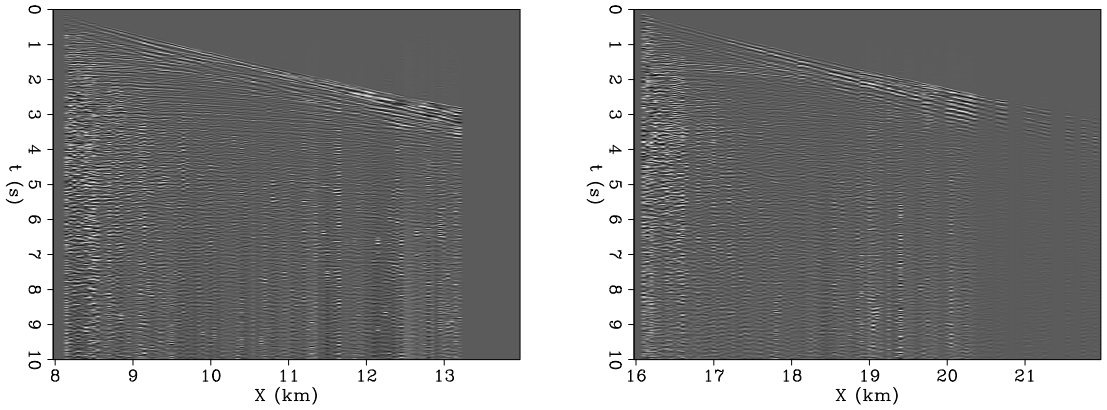

(a) (b)

Figure 3: Two sample shot gathers. [**ER**]

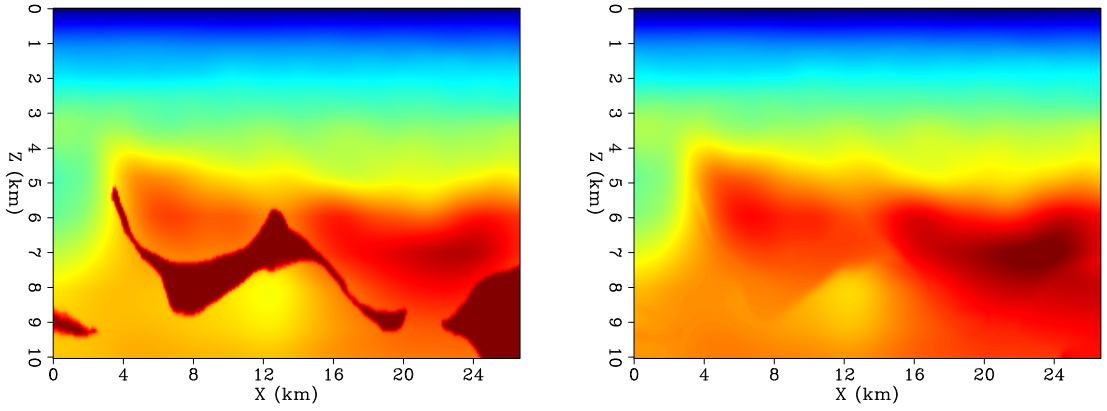

(a) (b)

Figure 4: On the left is the provided isotropic velocity model, obtained by ray-based tomography. On the right is the velocity model in which the salt bodies have been replaced with sediments. [**ER**]

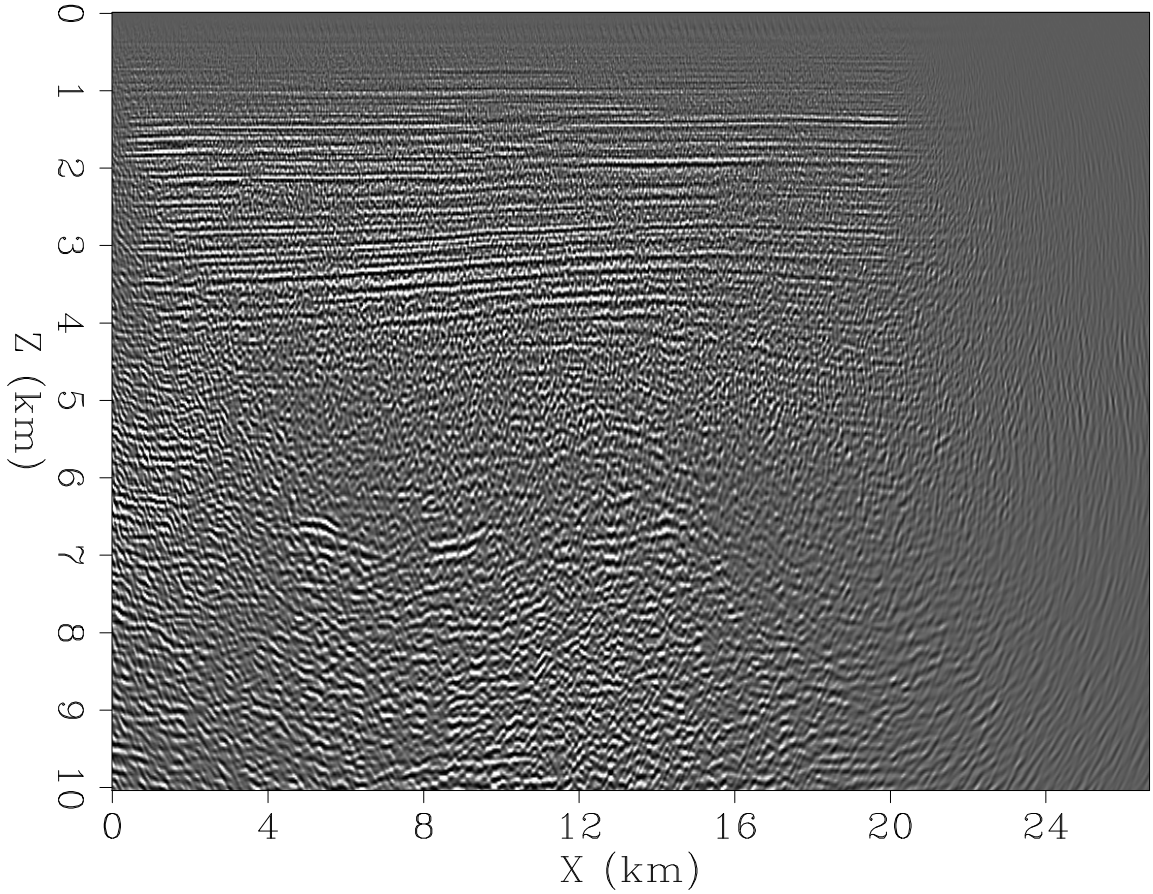

Figure 5: Migrated image with isotropic velocity model shown in Figure 4b shows sedimentary layers above four kilometers and segments of the salt boundaries at about seven kilometers. [**CR**]

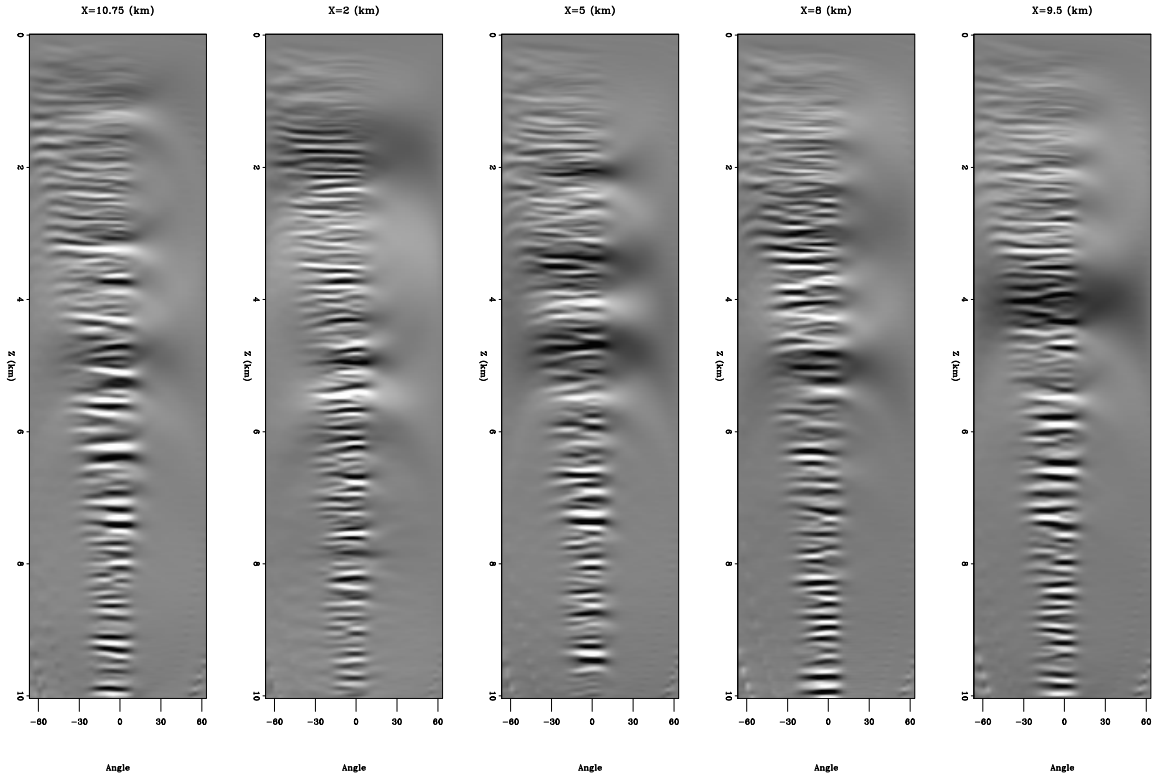

Figure 6: Angle gathers show downward curvatures at some locations, for example at five kilometers depth at $X = 10.75$ km and 4.5 km depth at $X = 2$ km. [**CR**]

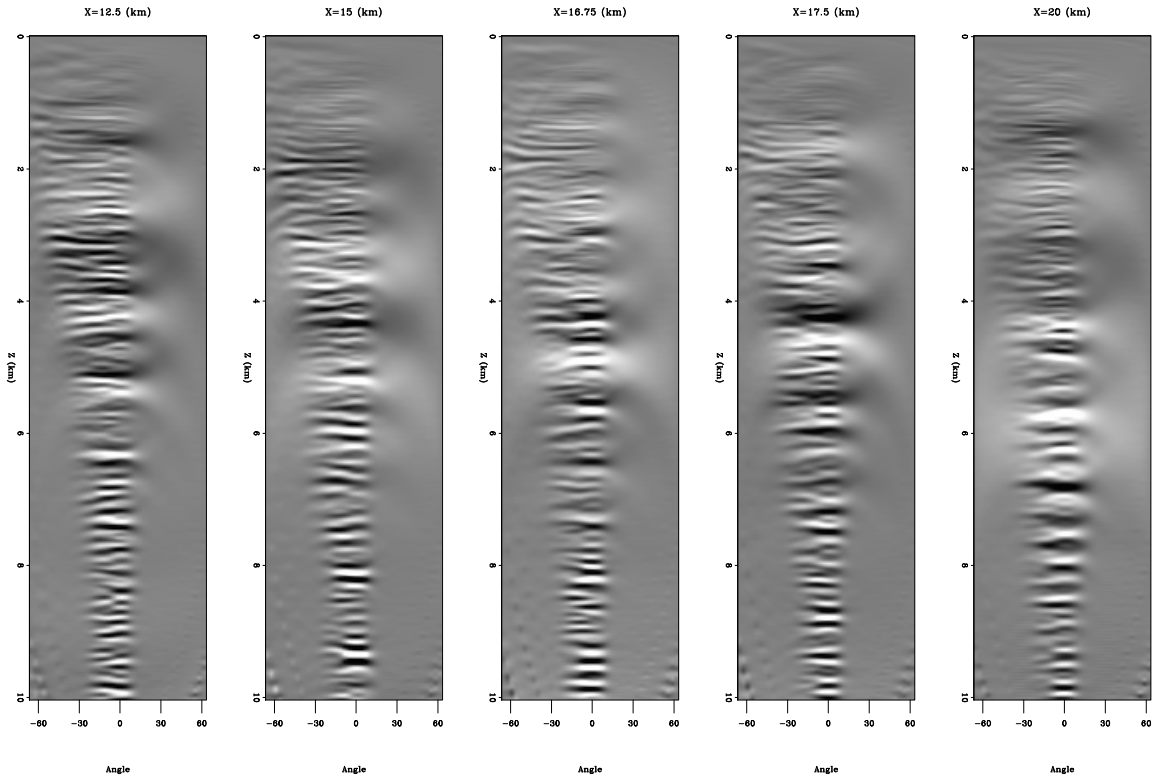

Figure 7: More angle gathers at various locations. [**CR**]

REFERENCES

Le, H., 2016a, Anisotropic full waveform inversion: SEP-Report, **163**, 155–162.

———, 2016b, Practical issues in anisotropic full waveform inversion: SEP-Report, **165**, 1–15.

Li, Y., B. Biondi, R. Clapp, and D. Nichols, 2016, Integrated VTI model building with seismic data, geological information, and rock-physics modeling-Part 1: Theory and synthetic test: Geophysics, **81**, C177–C191.